Characterization of iron in silicon by low-temperature photoluminescence and deep-level transient spectroscopy

Minoru Nakamura, Susumu Murakami, and Haruhiko Udono
College of Engineering, Ibaraki University, Hitachi, Ibaraki 316-8511, Japan

We investigate the relationship between the intensity of band-edge (BDE) photoluminescence (PL) from 10 to 70 K and the concentration of iron diffused in boron-doped p-type silicon. Because of the nonradiative recombination activity of the interstitial iron-boron complex (Fe_iB center), the BDE-PL intensity at each temperature varies distinctively and systematically with the iron concentration, which means that this method has the potential to make the accurate measurements of a wide range of interstitial iron concentrations in silicon. The iron precipitates formed in the bulk and/or at the surface are found to exert much weaker recombination activity for excess carriers than Fe_iB center by exploiting both PL and deep-level transient spectroscopy (DLTS) measurements. The unexpected enhancement in BDE-PL intensity from iron-diffused silicon between 20 and 50 K is attributed to the passivation of the Si-oxide/Si interface by iron. For the samples diffused with trace amounts of iron, the iron concentration within 20 μm of the surface is significantly greater than that in the bulk, as measured by DLTS. This result is tentatively attributed to the affinity of iron with the Si-oxide.
Published by AIP Publishing. https://doi.org/10.1063/1.5019958

I. INTRODUCTION

Since iron is ubiquitous and extremely detrimental for silicon devices, even at trace concentrations of $10^{10}-10^{11}$ cm^{-3}, because of its strong recombination activity with excess carriers,[1–3] numerous studies have been made on the behavior and properties of iron in silicon, as reviewed by several authors.[4–6] It is best to detect the contaminating metal while processing devices and to take immediate countermeasures to remove it. Deep-level transient spectroscopy (DLTS) is a sensitive and species-discriminating probe that is commonly used to detect the heavy-metal impurities in silicon.[5] In p-type silicon in which iron is diffused at high temperatures, dissolved interstitial iron (Fe_i) forms a complex with dopants that, after cooling the sample to room temperature, can be detected by DLTS.[5,7] The iron-boron complex (Fe_iB) has energy levels at $E_v + 0.10$ eV (E_v: the top energy of the valence band) as a donor center[7] and at $E_c - 0.29$ eV (E_c: the bottom energy of the conduction band) as an acceptor center.[8] The shortcomings of DLTS method are, however, laborious to prepare the samples (the formation of a p/n junction or a Schottky electrode) and destructive. Other sensitive and nondestructive approaches to detect iron are surface photo-voltage (SPV),[9] lifetime,[10] and photoluminescence (PL) measurements. Although iron shows no characteristic PL peak, PL may be used to detect the contaminating iron by exploiting the strong recombination activity of the iron complex. Actually, measuring the band edge (BDE) PL intensity at room temperature has already been used to characterize iron in multicrystalline silicon for solar cells.[11–13] Since the BDE-PL intensity for clean silicon samples at 10 K is over three orders of magnitude greater than at room temperature,[14] measurements of the BDE-PL at low temperatures might improve the accurate determination of impurity concentrations. In addition, low-temperature high-sensitivity PL measurements are expected to reveal new information about the actions of the impurity and its precipitates, which can be hardly obtained by room temperature measurements.

In the present study, we measure the low-temperature BDE-PL intensity as a function of iron concentration for p-type silicon diffused with a wide range of concentrations of iron. The PL intensity at each temperature shows a characteristic decrease with increasing iron concentration, which promises an accurate determination of the iron concentration. In addition, this technique reveals new information on the surface passivation by iron and recombination activity of the iron precipitates.

II. EXPERIMENT

The initial samples were 150-mm-diameter, 550-μm-thick (100) Czochralski-grown Si wafers doped with $1.1 \pm 0.2 \times 10^{15}$ cm^{-3} of boron (p-type) and mirror-polished on one side. Aqueous solutions containing iron were spin-coated onto the mirror-polished sides of the wafers to contaminate the wafers with iron.[15] Before contamination with iron, the wafer surfaces were made hydrophilic by washing in a HCl:H_2O_2:H_2O = 1:1:6 solution at $75 - 80$ °C, which means that a thin silicon oxide film formed on the surface. The wafers were contaminated with five surface concentrations of iron ($3.13 \pm 1.50 \times 10^{10}$ to $1.09 \pm 0.20 \times 10^{14}$ cm^{-2}), as measured by a commercial total-reflection X-ray fluorescence spectrometer (TRXF). These wafers are denoted F1–F5 in order of increasing iron concentration. The iron was allowed to diffuse into each wafer at 1000 °C for 30 min in a quartz furnace under clean, flowing dry nitrogen gas, following which they were cooled to room temperature by drawing them at a constant speed of 100 mm/min (average cooling rate ≈50 °C/min) to the mouth of the furnace. Since the thickness of silicon oxide is very thin [probably ≤1 nm (Ref. 15)] and the diffusivity of iron at 1000 °C in silicon is

approximately 10^{-5} cm^2/s,[4] the diffusion length of the metal in the wafer by the diffusion for 30 min is approximately 1.3 mm, which is sufficient for the metal to distribute homogeneously in the wafer. After cooling, the wafers were cut into numerous small chips (20×8 mm^2). A sample with no iron contamination (called the *reference sample*) was also prepared; it went through all the aforementioned processes except the contamination with iron. All these processes were carried out in a class 100 clean room.

The PL measurements were taken by using a standard luminescence setup, in which the samples were maintained at a constant temperature between 10 and 70 K in a mechanically cooled conduction type cryostat (DAIKIN, Cryo Kelvin) equipped with a temperature controller (Cryo-Con, model 32). Each sample was put into a caved ($21.0 \times 9.0 \times 2.0$ mm^3) copper holder ($40 \times 40 \times 3$ mm^3) after putting a soft indium sheet (50 μm) on the bottom of the cave and was covered by a copper spacer ($20.5 \times 8.5 \times 1.5$ mm^3) that has a hole (2.5 mmϕ) for laser irradiation and a hole (2.5×3.0 mm^2) for a thermometer. The spacer was covered by a copper plate ($40 \times 40 \times 1$ mm^3) having a window (3.0 mmϕ) for the laser excitation, and this plate together with the holder containing the sample was tightly fixed to the cold finger of the cryostat by four screws; that is, the sample was surrounded and pressed by the heat-conducting metals (In and Cu) except the small windows. The temperature of the sample was measured by a Si diode thermometer (LakeShore, model DT-670-SD) tightly attached on the sample surface by a screw near (within 0.5 mm) the window for laser irradiation. The thermometer was also used for controlling the sample temperature. The Au-plated copper radiation shields having small windows for laser irradiation and for PL observation were doubly surrounded around the sample holder. The samples were excited by a laser (wavelength: 532 nm, power: 10 mW, and spot diameter: 2 mmϕ) through an optical port of the cryostat with the back scattering geometry, and PL was detected by using a liquid-nitrogen-cooled Ge photodiode connected to a conventional lock-in amplifier to process the signal. The frequency of the light chopper was 50 Hz. Since the increase in temperature near the laser spot on the sample during the laser irradiation did not exceed 0.3 K at the lowest temperature (8.5 K) under the off-controlling condition of temperature, the increase in the temperature at the laser spot on the sample during laser irradiation is estimated to be controlled within 1 K at temperatures above 10 K, because of the small laser density (≈ 0.8 W/cm^2) and considerably high thermal conductivity of the sample. At least four samples (i.e., chips) cut from the same wafer were submitted.

The samples used for the PL measurements were next used for the DLTS measurements. The samples were first rinsed with 0.5% HF aqueous solution. Next, 1-mm-diameter, 100-nm-thick Ti Schottky barrier electrodes were formed on the Fe-diffused side of the samples by evaporation, following which a 1-μm-thick Al metal layer was deposited on each Ti electrode by evaporation. Before the DLTS measurements, each sample was characterized by capacitance-voltage measurements. The temperature-scan measurements were taken by using a commercial DLTS spectrometer (SEMILAB,

DLS-83D). The bias voltage was -5.0 V, and the forward pulse voltage determined from the bias voltage was $+4.0$ V. The lock-in frequency and pulse width were 244 Hz and 20 μs, respectively. Under these conditions, the analytical depths were estimated to be within 3.0 μm from the surface.[16] Each concentration of the Fe$_i$B center measured by DLTS was calibrated by the dopant concentration measured by the capacitance-voltage method. The detection limit of the DLTS system used in this study was approximately 5×10^{10} cm^{-3}.

III. RESULTS

A. Relationship between surface and bulk concentrations of iron

We first discuss the results of the DLTS measurements. In all the Fe-diffused samples, the DLTS signal peaks at approximately 50 K due to the Fe$_i$B donor center[7] (the spectrum not shown). No other peak appears in the spectrum. Figure 1 shows the bulk concentration of the Fe$_i$B center measured by DLTS as a function of the surface concentration of Fe measured by TRXF. The *expected concentration* of the Fe$_i$B center calculated by assuming homogeneous dissolution of all the contaminating iron atoms as the center is shown by a broken line. The solubility of iron at 1000 °C taken from previous works[4,6] is also shown. The measured bulk concentrations of the Fe$_i$B center for the samples with surface concentrations of iron between 1.17×10^{12} (sample F3) and 1.43×10^{13} cm^{-2} (sample F4) fall on the expected-concentration line, indicating that most of the iron dissolves homogeneously as Fe$_i$B in this range of surface concentration and does not form precipitates, even given the very slow cooling rate. This is consistent with the lack of iron precipitation when the concentration of iron is less than or near the solubility of the metal.[17] However, outside this range of surface concentration, the Fe$_i$B concentration departs from the expected-concentration line. The Fe$_i$B concentration for the sample with the highest surface concentration (F5) is clearly less than the solubility of iron at 1000 °C. Because iron does not evaporate at the diffusion temperature,[15] all
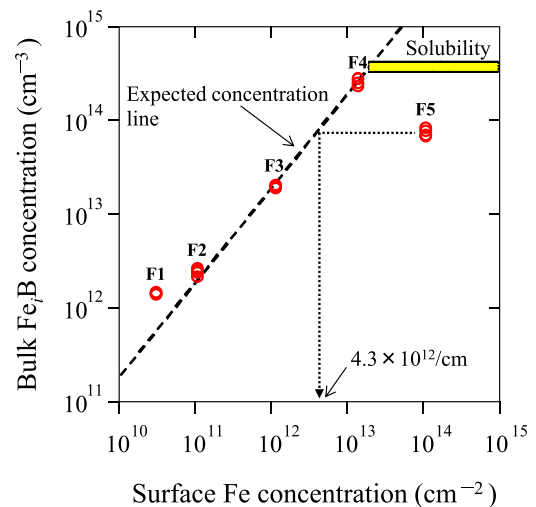

FIG. 1. Bulk concentration of Fe$_i$B as a function of surface concentration of iron. Bulk concentration was measured by DLTS and surface concentration of iron was measured by TRXF.

contaminating iron atoms remain in the bulk and/or on the surface in these experiments. This unexpectedly low concentration of Fe$_i$B in sample F5 is attributed to the formation of precipitates because (i) the surface concentration of contaminating iron for sample F5 exceeds the solubility of iron when it is completely dissolved at the diffusion temperature, and (ii) no iron species other than Fe$_i$B appears in the DLTS spectrum of the sample. When the dissolution of iron is limited by the solubility of the metal at the diffusion temperature, the iron remaining on the surface may nucleate during cooling.[18] Iron is also known to easily precipitate in the bulk when the bulk-iron concentration is sufficiently high ($\geq 5 \times 10^{13}$ cm^{-3}).[2] Based on the expected-concentration line, the average bulk concentration of the Fe$_i$B for sample F5 is estimated to correspond to a surface concentration of iron 4.3×10^{12} cm^{-2}, as indicated by the dotted line in Fig. 1.

Conversely, for surface concentrations of iron less than 1.17×10^{12} cm^{-2}, the Fe$_i$B concentration exceeds the expected concentration. To investigate this unexpected concentration, the surface of sample F1 was etched to appropriate depths by a HF/HNO$_3$ aqueous solution and the Fe$_i$B concentration was measured by DLTS. With approximately 20 μm etched off, the concentration of the Fe$_i$B center no longer exceeds the expected concentration ($\approx 5.7 \times 10^{11}$ cm^{-3}), indicating that the higher concentration initially observed is localized within 20 μm of the surface. This finding is consistent with that of Nauk and Gometz,[19] who showed that the Fe$_i$B concentration near the surface is far larger than in the bulk (i.e., more than approximately 20 μm from the surface) for dilute-Fe-diffused samples. The localization of excess iron near the surface has also been reported in several other papers.[17,20,21] This finding may result from (i) the affinity of surface oxide film to iron,[22,23] and (ii) the low diffusivity of iron in the oxide, which may prevent out-diffusion of iron and accumulate it at the Si-oxide/Si interface while the sample is cooled. The excess iron concentration near the sample surface may be the case for all samples with higher Fe concentration; however, such excess concentration was not clearly observed in this study, probably because it is always much less than the total concentration of the Fe$_i$B center measured.

B. Changes in PL spectrum with temperature and iron concentration

Figure 2 shows BDE-PL spectra for several temperatures for the reference sample (all measurement conditions other than temperature were held fixed). The PL peaks due to the phonon replicas of free exciton (FE) and boron-bound exciton (BE) recombination are denoted by using the notation of Kosai and Gershenzon,[24] where "TO" and "TA" indicate transverse optical and transverse acoustic phonons, respectively. The symbol Γ indicates a TO phonon replica at the Γ point, and B* indicates the boron-related peak. The intensities of the BE-related peaks rapidly decrease with increasing temperature. When the temperature is raised to 25 K, the BE-related peaks almost disappear. Each peak broadens with increasing temperature, which indicates that
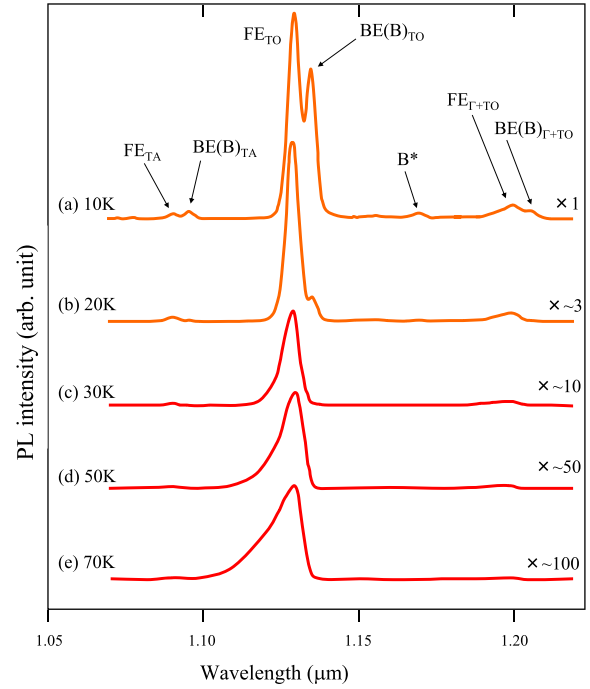

FIG. 2. PL spectra of the reference sample for several temperatures. Temperatures and magnifications are given in the figure.

the integral of the peak should be used as intensity to evaluate the temperature dependence of the PL intensity.

Figure 3 shows BDE-PL spectra for samples F1 − F5 and for the reference sample measured at 10 K. Although the
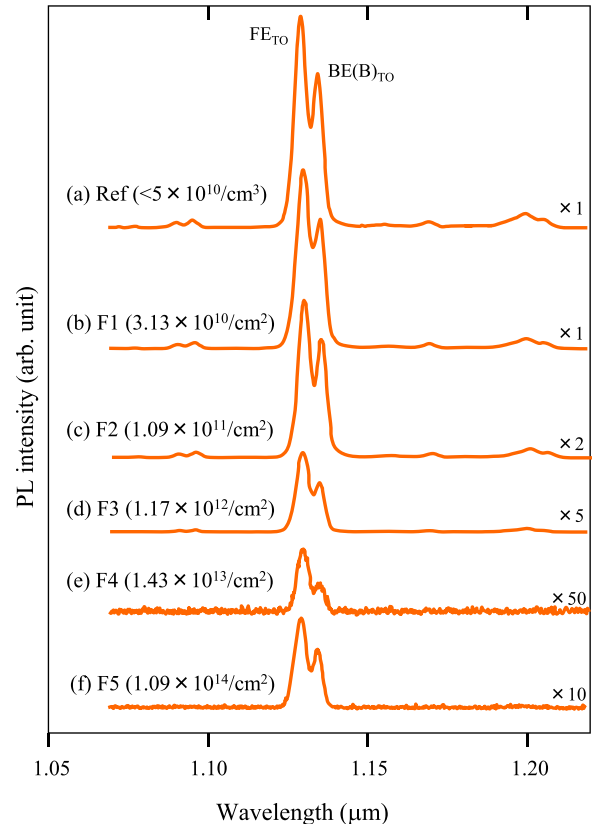

FIG. 3. PL spectra for several iron concentrations at 10 K. Sample names, iron concentrations, and magnifications are given in the figure. Ref indicates the reference sample.

iron surface concentration strongly influences peak intensity, it has very little influence on the shape of the spectra. The relative decrease in the intensity of the BE_{TO} peak compared with that of the FE_{TO} peak, which is due to the decrease in neutral boron concentration[25] as a result of Fe_iB formation, barely appears only for sample F4.

C. PL intensity dependence on iron concentration

Figure 4 shows the PL intensity as a function of surface concentration of iron for eight different temperatures. Because the PL intensity of the TA phonon replica and of the two-phonon replicas is sufficiently small, the intensity is defined as the sum of the integrated intensities of the TO phonon replicas of the FE and BE peaks. Each data point reveals the average of the PL intensities for at least four samples. The bulk concentration of iron calculated by assuming homogeneous dissolution of all the contaminating iron atoms is drawn on the top axis. At each temperature, the PL intensity decreases monotonically with increasing iron concentration from $3.13 \times 10^{10} \, \text{cm}^{-2}$ (sample F1) to $1.43 \times 10^{13} \, \text{cm}^{-2}$ (sample F4) and increases again at $1.09 \times 10^{14} \, \text{cm}^{-2}$ (sample F5). The decrease in the PL intensity with increasing iron concentration is clearly due to nonradiative recombination of excess carriers by Fe_iB. The upturn in PL intensity for sample F5 is attributed to the decrease in Fe_iB concentration, which in turn is due to the precipitation of iron in the bulk and on the surface, as explained earlier.

The surface Fe concentration, which determines the PL intensity of sample F5 is estimated by equating the PL intensity of the sample to that of the un-precipitated sample, as shown by the dotted line for each temperature in Fig. 4. The average surface concentration of Fe obtained from the PL data between 10 and 30 K is $4.5 \pm 0.3 \times 10^{12} \, \text{cm}^{-2}$, which is consistent with the surface concentration of $4.3 \times 10^{12} \, \text{cm}^{-2}$ determined by DLTS. Based on this result, we infer that only

the Fe_iB concentration determines the PL intensity and that the iron precipitates exert much weaker recombination activity for excess carriers than the Fe_iB center, although the precipitate is known to have an obvious recombination activity.[26] This inference is consistent with the result that the iron precipitates are less harmful than the interstitial iron (including Fe_iB) in the solar cells fabricated with multicrystalline silicon.[27]

Summarizing these results, the concentrations of the harmful Fe_iB in a sample can be determined by exploiting the data shown in Fig. 4 for appropriate temperatures, even when the iron precipitates are formed. When the data around $10 - 15 \, \text{K}$ are used, the concentrations of Fe_iB from approximately 1×10^{11} to $1 \times 10^{14} \, \text{cm}^{-3}$ can be determined with high sensitivity. However, based on the data measured at temperatures higher than 70 K, the quantitative determination of Fe_iB concentrations greater than approximately $10^{12} \, \text{cm}^{-3}$ is rather difficult, because the PL intensity becomes extremely small at these temperatures. Thus, the PL method explained in this study has the potential to generally make the accurate measurements of a wide range of interstitial iron concentrations in silicon by exploiting the PL calibration curves measured at appropriately low temperatures. However, since the systems and conditions for PL measurements are different in different laboratories, proper calibration curves using several standard samples should be obtained in each laboratory. The extension of the PL method to the measurements of other metal impurities is discussed. Since other heavy metals, such as Ni and Cu, are not known to form clear recombination centers due to the formation of dopant/metal complexes in Czochralski-grown silicon, however, the measurement of these metals by applying the PL method mentioned above seems difficult; that is, the strong recombination activity mentioned above is specific for iron/ acceptor combination.

IV. DISCUSSION

A. Actions of iron

The inspection of Fig. 4 reveals a strange feature: The PL intensity of the reference sample is less than that of sample F1 in the low-temperature region. Figure 5 shows the PL intensity of each sample as a function of temperature. For the sake of brevity, the data for the precipitated sample (F5) are not shown. This figure clearly shows that the PL intensity of sample F1 exceeds that of the reference sample from 20 to 50 K. The BDE-PL intensity I_{PL} due to steady-state excitation is[28]

$$I_{PL} = \alpha G_L \left[\tau_r^{-1} / (\tau_r^{-1} + \tau_{nr}^{-1}) \right], \quad (1)$$

where α is the fraction of the BDE-PL intensity and G_L is the rate at which excess carriers are generated by photoexcitation. The quantities τ_r and τ_{nr} are the radiative and nonradiative recombination time constants of excess carriers, respectively. The quantity τ_{nr}^{-1} contains a contribution from the bulk $(\tau_{nr,B}^{-1})$ and from the surface $(\tau_{nr,S}^{-1})$

$$\tau_{nr}^{-1} = \tau_{nr,B}^{-1} + \tau_{nr,S}^{-1}. \quad (2)$$
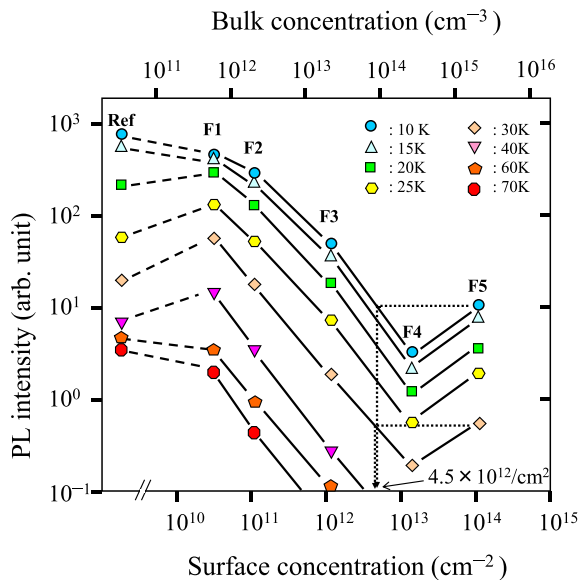

FIG. 4. PL intensity as a function of surface concentration of iron for several temperatures. Ref indicates the reference sample.
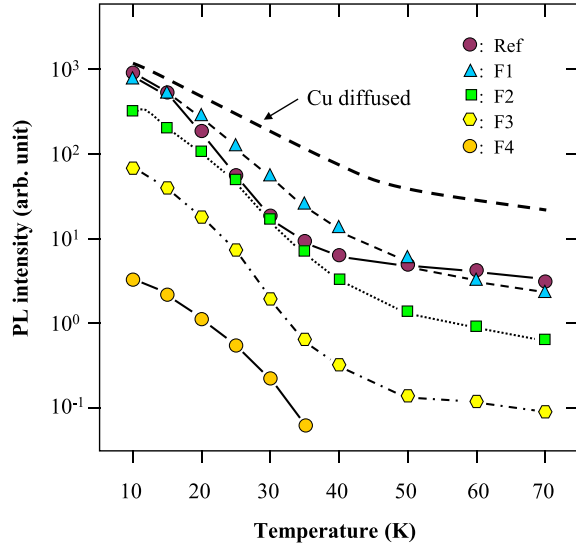
FIG. 5. PL intensity as a function of temperature for the reference sample and Fe-diffused samples F1−F4. The dashed line shows the PL intensity of a Cu-diffused sample.

Because the term τ^{-1} multiplied by the excess carrier concentration gives the recombination rate for each process,[29] τ_r^{-1}, $\tau_{nr,B}^{-1}$, and $\tau_{nr,S}^{-1}$ in Eqs. (1) and (2) can be replaced by the recombination rates U_r, $U_{nr,B}$ and $U_{nr,S}$, respectively. In silicon, the radiative recombination rate is much less than the nonradiative recombination rate when the surface of the sample is not passivated,[30] so I_{PL} is dominated by $U_{nr,B}$ and $U_{nr,S}$ for all Fe-diffused samples in this study. The recombination rate $U_{nr,B}$ contains the contributions from Auger ($U_{nr,Auger}$), thermal quenching ($U_{nr,Th}$),[28] and defect recombination ($U_{nr,D}$).[28,29] However, for the present work, $U_{nr,Auger}$ may be neglected because this process is important only for heavily doped samples and/or samples injected with a large concentration of excess carriers.[12,29] $U_{nr,Th}$ is defined to explain the decrease in the PL intensity caused by multiphonon processes, which increase with increasing temperature.[28] This rate is assumed to be the same at any given temperature for all the samples used in this study. Because the samples used herein contain no bulk recombination defect other than Fe$_i$B, $U_{nr,D}$ is entirely due to this center and is well expressed by the model proposed by Shockley and Read,[31] and Hall[32] (SRH model). $U_{nr,S}$ is due to the surface traps or interfacial traps at the Si-oxide/Si interface.[29] Whereas the PL intensity of sample F1 is dominated by $U_{nr,D}$, $U_{nr,Th}$, and $U_{nr,S}$, that of the reference sample is dominated by $U_{nr,Th}$ and $U_{nr,S}$, because this sample is assumed to contain no bulk defects. Accordingly, the aforementioned predominance in PL intensity of sample F1 with respect to the reference sample from 20 to 50 K is attributed to a smaller $U_{nr,S}$ in sample F1 because $U_{nr,Th}$ is the same for both samples.

We now discuss the origin of the decrease in $U_{nr,S}$ in sample F1. Based on the known enhancement of the BDE-PL intensity due to the passivation by copper of interfacial traps at a Si-oxide/Si interface,[14] approximately 5×10^{13} cm^{-2} of copper was diffused at 700 °C in the same series wafer as used herein for iron diffusion, with the method reported

previously.[14] Figure 5 shows the PL intensity of the Cu-diffused sample (dashed line). The PL intensity of this sample is generally greater than that of the reference sample and sample F1 over the entire range of temperature investigated. This predominance is attributed to the excellent passivation of interfacial traps by copper in the sample containing no bulk defects.[14] Based on the similar behavior of the PL intensities for both sample F1 and the Cu-diffused sample, the decrease in $U_{nr,S}$ in sample F1 is suggested to occur by the passivation of interfacial traps by iron. The main reasons for the PL intensity of sample F1 is always less than that of the Cu-diffused sample are (i) the influence of $U_{nr,D}$ which is due to the formation of Fe$_i$B in sample F1 and (ii) probably the less effective passivation activity of iron compared to copper. To confirm the iron passivation, we etched off approximately 20 μm of the surfaces of the three samples (F1, reference, and Cu-diffused) in a HF/HNO$_3$ solution, with the same method reported previously.[14] Then, we immersed these samples in conc. HNO$_3$ for 24 h to form a new oxide on each sample surface to annihilate the effect of the hydrogen passivation of the surface[33,34] caused by the immersion of the solution. After rinsing and drying the samples, we measured the PL intensities of these samples. Whereas the PL intensities of the etched reference sample and etched Cu-diffused sample were almost the same as the intensity of the unetched reference sample, the intensity of the etched sample F1 was slightly lower than the unetched reference sample over the entire range of temperature investigated; that is, the increase in the PL intensity of sample F1 is confirmed to attribute to the passivation of interfacial traps by iron. It is clear that the PL intensities of other samples contaminated with higher concentrations of iron are also influenced by both bulk recombination by Fe$_i$B and surface passivation by iron. Surface passivation by metals, such as nickel[35] and iron,[36] in porous silicon is well known, although the passivating activities of the two metals are rather different. A detailed investigation of the bonding structures of copper, nickel, and iron at the interface of Si-oxide/Si is left for future work.

We now calculate the elementary recombination rates for a p-type Czochralski-grown sample to explain the predominance of the PL intensity of sample F1 over that of the reference sample from 20 to 50 K. The elementary bulk SRH recombination rate $R_{B,SRH}$ (cm^{-3} s^{-1}) of excess carriers comes from a trap with an energy level at E_t in the band-gap and is expressed as[29]

$$R_{B,SRH} = \sigma_p \sigma_n v_{th} N_t [pn - n_i^2] / \{\sigma_n[n + n_i \exp(E_t - E_i)/kT]$$
$$+ \sigma_p[p + n_i \exp(E_i - E_t)/kT]\}, \quad (3)$$

where σ_p, σ_n, v_{th}, and N_t are the hole cross section, electron cross section, thermal velocity of carriers, and trap concentration, respectively. The quantities p, n, n_i, E_i, k, and T are the hole concentration, electron concentration, intrinsic carrier concentration, electron energy at the intrinsic Fermi level, Boltzmann constant, and absolute temperature, respectively. The trap level at $E_c - 0.26$ eV [or $E_c - 0.29$ eV (Ref. 8)] for Fe$_i$B is the most effective nonradiative recombination trap in p-type silicon.[37] When no bulk defects other than

Fe$_i$B are present, $U_{\text{nr,D}}$ may be approximated by $R_{\text{B,SRH}}$ for this trap.[29]

The elementary surface SRH recombination rate $R_{\text{S,SRH}}$ $(\text{cm}^{-2}\,\text{s}^{-1})$ comes from an interfacial trap with an energy level at E_t and is expressed as[29]

$$R_{\text{S,SRH}} = \sigma_\text{p}\sigma_\text{n}v_{\text{th}}N_{it}\left[p_s n_s - n_i^2\right]/\{\sigma_\text{n}[n_s + n_i \exp(E_t - E_i)/kT] + \sigma_\text{p}[p_s + n_i \exp(E_i - E_t)/kT]\}, \quad (4)$$

where N_{it}, p_s, and n_s, are the concentration of interfacial traps, the surface hole concentration, and the surface electron concentration, respectively, and are formally transferred from N_t, p, and n, respectively, which appear in Eq. (3). The temperature dependence of $R_{\text{S,SRH}}$ (or $R_{\text{B,SRH}}$) for different trap energies E_t appears in Fig. 6, in which the constants used in the calculation are indicated in the figure. Because the traps other than Fe$_i$B are hypothetical, the value of σ_n ($\sim 2.5 \times 10^{-15}\,\text{cm}^2$)[38] for the Fe$_i$B level at $E_c - 0.26\,\text{eV}$ is used for all σ in the figure assuming that they are independent of temperatures. When the excess carrier concentrations are below $1 \times 10^{15}/\text{cm}^3$, as are the cases herein and the PL imasing,[12] the features shown in Fig. 6 are not greatly altered. As shown in Fig. 6, when E_t is near the conduction-band edge, $R_{\text{S,SRH}}$ (or $R_{\text{B,SRH}}$) is a maximum at low temperature and sharply decreases with increasing temperature. Taking into account this trend, a decrease in the concentration of traps with energies near the conduction-band edge is expected to lead to a decrease in $R_{\text{S,SRH}}$ at low temperatures and to enhance the PL intensity in that region. For an actual sample, because the interfacial trap levels are distributed throughout the band-gap and their density is given by the well-known U-shaped continuum, $D_{it}(E_t)$[39] $(\text{cm}^{-2}\,\text{eV}^{-1})$, the single-trap SRH recombination rate given in Eq. (4) should be replaced by an integration over the band-gap for $D_{it}(E_t)$ as[40]

$$R'_{\text{S,SRH}} = \sigma_\text{p}\sigma_\text{n}v_{\text{th}}\left[p_s n_s - n_i^2\right]$$
$$\times \int_{E_v}^{E_c} D_{it}(E_t)dE_t/\{\sigma_\text{n}[n_s + n_i \exp(E_t - E_i)/kT] + \sigma_\text{p}[p_s + n_i \exp(E_i - E_t)/kT]\}. \quad (5)$$

Although $U_{\text{nr,S}}$ is in general a complicated function of $R'_{\text{S,SRH}}$, the diffusion constant of carriers, and the sample thickness d,[41] $U_{\text{nr,S}}$ may be approximated by $2R'_{\text{S,SRH}}/d$ for an ordinarily thick ($0.1\,\text{mm} \le d \le 1\,\text{mm}$) wafer,[29,42] when $R'_{\text{S,SRH}}$ is sufficiently small, as is assumed herein. Because the density $D_{it}(E_t)$ near the conduction- and valence-band edges is several orders of magnitude greater than that around the band center,[43,44] a reduction in $D_{it}(E_t)$ enhances the PL intensity in the low-temperature region more effectively than in the higher temperature region, when σ are independent of temperatures and trap energies. The aforementioned predominance in the PL intensity of sample F1 over that of the reference sample in that temperature region is explained by the fact that (i) $U_{\text{nr,S}}$ (or D_{it}) is reduced in sample F1 due to the passivation of interfacial traps by iron and (ii) that the bulk recombination rate $U_{\text{nr,D}}$ due to Fe$_i$B is not too large in the low-temperature region. With increasing temperature, the surface recombination, which comes from the U-shaped $D_{it}(E_t)$, affects the PL intensity more weakly and the bulk recombination, which comes from Fe$_i$B, affects the PL intensity more strongly as can be seen from Fig. 6. This leads to the expectation that the PL intensity of sample F1 crosses over that of the reference sample at a higher temperature (near 50 K in Fig. 5).

V. SUMMARY

We measured the BDE-PL intensity as a function of iron concentration in silicon from 10 to 70 K. At each temperature, the BDE-PL intensity varies distinctively and systematically with iron concentration because of the intense recombination activity of the Fe$_i$B center. The iron precipitates that form in the bulk and/or at the surface are found to exert much weaker recombination activity for excess carriers than the Fe$_i$B center. From these results, the PL method is suggested to have the potential to accurately determine a wide range of interstitial iron concentrations by selecting appropriate calibration curves measured at various low-temperatures. For the sample diffused with trace amounts of iron, the concentration of iron within 20 μm of the surface is clearly greater than that deeper in the bulk, as determined by DLTS. This result is tentatively attributed to the affinity of iron to the Si oxide at the sample surface. From 20 to 50 K, the BDE-PL intensity from the iron-diffused sample F1 exceeds that of the reference sample, which is attributed to the competitive effects between (i) enhanced PL intensity due to surface passivation by iron and (ii) reduced intensity due to nonradiative bulk recombination by the Fe$_i$B center.
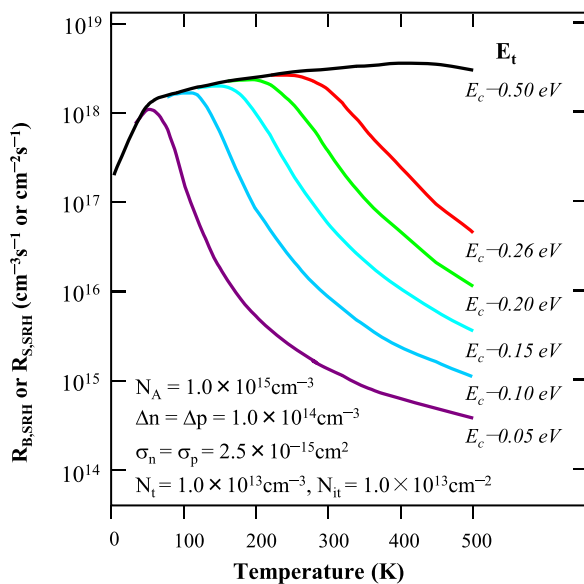

FIG. 6. Recombination rate as a function of temperature and for several trap levels E_t. The parameters used are shown in the figure. N_A is the acceptor concentration, and Δp and Δn are the excess concentrations of holes and electrons, respectively.

[1]A. Rohatgi, J. R. Davis, R. H. Hopkins, and P. G. McMullin, Solid-State Electron. **26**, 1039 (1983).

[2]A. Kaniava, E. Gaubas, J. Vaitkus, J. Vanhellemonto, and A. L. P. Rotondaro, Mater. Sci. Technol. **11**, 670 (1995).

[3]J. E. Birkholz, K. Bothe, D. Macdonald, and J. Schmidt, J. Appl. Phys. **97**, 103708 (2005).

[4]E. R. Weber, Appl. Phys. A **30**, 1 (1983).

[5]K. Graff, *Metal Impurities in Silicon-Device Fabrications* (Springer, Berlin, 1995).

[6]A. A. Istratov, H. Hieslmair, and E. R. Weber, Appl. Phys. A **70**, 489 (2000).

[7]K. Graff and H. Pieper, J. Electrochem. Soc. **128**, 669 (1981).

[8]S. D. Brotherton, P. Bradley, and A. Gill, J. Appl. Phys. **57**, 1941 (1985).

[9]G. Zoth and W. Bergholz, J. Appl. Phys. **67**, 6764 (1990).

[10]D. H. Macdonald, L. J. Geerligs, and A. Azzizi, J. Appl. Phys. **95**, 1021 (2004).

[11]T. Trupke, R. A. Bardos, M. C. Schubert, and W. Warta, Appl. Phys. Lett. **89**, 044107 (2006).

[12]D. Macdonald, J. Tan, and T. Trupke, J. Appl. Phys. **103**, 073710 (2008).

[13]A. Y. Liu and D. Macdonald, J. Appl. Phys. **115**, 114901 (2014).

[14]M. Nakamura and S. Murakami, Jpn. J. Appl. Phys., Part 1 **49**, 061301 (2010).

[15]M. Hourai, T. Naridomi, Y. Oka, K. Murakami, S. Sumita, N. Fujino, and T. Shiraiwa, Jpn. J. Appl. Phys., Part 2 **27**, L2361 (1988).

[16]M. Nakamura and S. Murakami, J. Appl. Phys. **111**, 073512 (2012).

[17]S. Sadamitsu, A. Sasaki, M. Hourai, S. Sumita, and N. Fujino, Jpn. J. Appl. Phys., Part 1 **30**, 1591 (1991).

[18]J. D. Murphy and R. J. Falster, J. Appl. Phys. **112**, 113506 (2012).

[19]K. Nauka and D. A. Gometz, J. Electrochem. Soc. **142**, L98 (1995).

[20]Y. Kamiura, F. Hashimoto, and M. Iwami, Appl. Phys. Lett. **53**, 1711 (1988).

[21]X. Gao, H. Mollenkopf, and S. Yee, Appl. Phys. Lett. **59**, 2133 (1991).

[22]T. Kitano, J. Electron. Mater. **21**, 1027 (1992).

[23]M. Takiyama, S. Ohtsuka, S. Hayashi, and M. Tachimori, in *Semiconductor Silicon 1994*, edited by H. R. Huff, W. Bergholz, and K. Sumino (Electrochemical Society, Pennington, 1994), p. 346.

[24]K. Kosai and M. Gershenzon, Phys. Rev. B **9**, 723 (1974).

[25]I. Broussell, V. A. Karasyuk, and M. L. W. Thewalt, Appl. Phys. Lett. **78**, 3070 (2001).

[26]P. Gundel, M. C. Schubert, F. D. Heinz, W. Kwapil, W. Warta, G. Martinez-Criado, M. Reiche, and E. R. Weber, J. Appl. Phys. **108**, 103707 (2010).

[27]D. Macdonald, A. Cuevas, A. Kinomura, Y. Nakano, and L. J. Geerling, J. Appl. Phys. **97**, 033523 (2005).

[28]I. Pelant and J. Valenta, *Luminescence Spectroscopy of Semiconductors* (Oxford University Press Inc., New York, 2011), Chaps. 3–6.

[29]D. K. Schroder, *Semiconductor Materials and Device Characterization* (John Wiley and Sons, New York, 2006), Chaps. 5–7.

[30]T. Trupke, J. Zhao, A. Wang, R. Corkish, and M. A. Green, Appl. Phys. Lett. **82**, 2996 (2003).

[31]W. Shockley and W. T. Read, Phys. Rev. **87**, 835 (1952).

[32]R. N. Hall, Phys. Rev. **87**, 387 (1952).

[33]E. Yablonovitch, D. L. Allara, C. C. Chang, T. Gmitter, and T. B. Bright, Phys. Rev. Lett. **57**, 249 (1986).

[34]T. Konishi, T. Yao, M. Tajima, H. Ohshima, H. Ito, and T. Hattori, Jpn. J. Appl. Phys., Part 2 **31**, L1216 (1992).

[35]S. Amdouni, M. Rahmani, M.-A. Zaibi, and M. Oueslati, J. Lumin. **157**, 93 (2015), and references therein.

[36]A. Mabrouk, N. Lorrain, M. L. Haji, and M. Oueslati, Superlattices Microstruct. **77**, 219 (2015), and references therein.

[37]Y. Hayamizu, T. Hamaguchi, S. Ushio, T. Abe, and F. Shimura, J. Appl. Phys. **69**, 3077 (1991).

[38]S. Rein and S. W. Glunz, J. Appl. Phys. **98**, 113711 (2005).

[39]S. M. Sze, *Physics of Semiconductor Devices*, 2nd ed. (Wiley, New York, 1981), Chap. 7.

[40]S. W. Glunz, A. B. Sproul, W. Warta, and W. Wettling, J. Appl. Phys. **75**, 1611 (1994).

[41]Y. Ogita, J. Appl. Phys. **79**, 6954 (1996).

[42]S. K. Pang and A. Rohatgi, J. Appl. Phys. **74**, 5554 (1993).

[43]N. M. Johnson, D. K. Biegelsen, M. D. Moyer, S. T. Chang, E. H. Poindexter, and P. J. Caplan, Appl. Phys. Lett. **43**, 563 (1983).

[44]M. J. Uren, J. H. Stathis, and E. Cartier, J. Appl. Phys. **80**, 3915 (1996).